Molecular-orbital description of doubly excited atomic states generalized to arbitrary dimension

J. M. Rost,* S. M. Sung, and D. R. Herschbach
Department of Chemistry, Harvard University, Cambridge, Massachusetts 02138

J. S. Briggs
Fakultät für Physik, Albert-Ludwigs-Universität, D-7800 Freiburg, Germany
(Received 23 December 1991)

The molecular-orbital description of two-electron atoms [J. M. Feagin and J. S. Briggs, Phys. Rev. A **37**, 4599 (1988)], derived from H_2^+ by interchanging the roles of electrons and nuclei, is generalized to D dimensions. For H_2^+ itself there exist myriad exact interdimensional degeneracies because $D \rightarrow D+2$ is equivalent to $m \rightarrow m+1$, augmenting by unity the projection of the electronic angular momentum on the internuclear axis. When the molecular orbitals (MO's) are transcribed to treat two-electron motion, additional constraints limit the exact degeneracies to states in $D=3$ and 5, but many approximate degeneracies persist. Since the MO description emphasizes rotational properties of the two-electron atom, the link between dimension and orbital angular momentum is a pervasive feature. We use this link to classify groups of quasidegenerate doubly excited atomic energies and to explain striking similarities among certain pairs of hyperspherical or molecular-orbital two-electron potential curves.

PACS number(s): 31.50.+w, 31.20.Gm

I. INTRODUCTION

Recalcitrant problems often can be better understood when recast as analogs of more accessible prototypes. This is the motivation for relating highly correlated states of a two-electron atom to a molecular counterpart, the H_2^+ molecule ion. The adiabatic molecular-orbital description of two-electron atoms [1] has elucidated both qualitative and quantitative features of the atomic spectra via parallels with the molecule [2]. Thereby the separability of the H_2^+ problem can be exploited to characterize symmetries of the atomic states. A kindred approach has proven useful even for the one-electron case, in relating spheroidal eigenfunctions of the hydrogen atom to its hidden symmetry [3]. In this paper, we extend the molecular-orbital (MO) description to arbitrary spatial dimensions, and thus facilitate a more comprehensive interpretation of two-electron spectra.

The adiabatic MO approach and D-dimensional generalization are naturally complementary, since both emphasize the rotational properties of a system. The MO description defines a set of body-fixed angular-momentum quantum numbers [2], and the D-dimensional generalization leads to a direct correspondence between angular momentum and spatial dimension [4]. In addition, both the MO description and dimensional treatment are associated with degeneracies in the H_2^+ molecular-orbital curves. Generalization to arbitrary dimension results in H_2^+ interdimensional degeneracies [4], and motion near the saddle region of the two-center Coulomb potential corresponds to approximate "saddle" degeneracies [2]. Thus it seems promising to combine the two approaches in addressing the two-electron atomic problem.

Because of their pronounced collective electron motion, the two-electron doubly excited states are fundamental in understanding the dynamics of electron correlation. Herrick and co-workers first noticed the rovibrational character of two-electron doubly excited states [5] and subsequently described the quasidegenerate spectra in terms of multiplet structure [6]. Yuh *et al.* also used the rovibrational model to interpret the angular correlations contained in configuration-interaction wave functions [7]. In addition, an alternative to the rovibrational model, the hyperspherical approximation, has been used to illustrate many qualitative features of the correlated electron motion of two-electron atoms [8] and, recently, to obtain quantitative results [9]. The adiabatic molecular treatment of two-electron atoms is distinct from these methods because it extracts an internal quantization axis directly from the Hamiltonian.

Previously, Lin [10] noticed similarities in the hyperspherical curves for states of different symmetries. Goodson *et al.* [11] attributed these similarities to interdimensional degeneracies of two-electron atoms, including some exact degeneracies proven by Herrick [12]. Some further approximate interdimensional degeneracies among doubly excited states have also been noted [13]. In this paper, we provide an explanation for the similarities of the two-electron adiabatic hyperspherical potentials and the degeneracies by emphasizing their molecular foundation. Essentially, we will show that the similar two-electron hyperspherical curves are based on molecular orbitals which correspond to dimensionally related pairs of H_2^+ states. We also illustrate how doubly excited atomic energy levels associated with saddle degeneracies can be approximated from D-dimensional $^1S^e$ energies. The D-dimensional energies have been calculated using dimensional perturbation theory [14].

Before developing the details of this correspondence, we first examine H_2^+. In Sec. II, after describing the D-dimensional H_2^+ problem and its exact interdimensional degeneracies, we identify the approximate degeneracies

associated with localized motion about the saddle point of the two-center potential. Section III focuses on linking H_2^+ molecular orbitals to doubly excited states of the two-electron atom and derives the D-dimensional generalization of the adiabatic MO method. In Sec. IV, we show how doubly excited atomic energies in $D=3$ can be organized into multiplets using the single-channel molecular approximation in D dimensions. Finally, in Sec. V we explain the observed similarities among pairs of hyperspherical two-electron curves using the D-dimensional molecular description. We also show how exact interdimensional degeneracies associated with H_2^+ are altered in the D-dimensional MO treatment of electron motion.

II. TWO-CENTER COULOMB PROBLEM IN D DIMENSIONS

A. Quantum numbers and exact degeneracies

The Hamiltonian for H_2^+ in D-dimensional cylindrical coordinates is defined by [4]

$$h^{\mathrm{TC}}=-\frac{1}{2}\left[\frac{1}{\rho^{D-2}}\frac{\partial}{\partial\rho}\rho^{D-2}\frac{\partial}{\partial\rho}+\frac{\partial^2}{\partial z^2}-\frac{l_{D-2}^2}{\rho^2}\right]+V(\rho,z)\ , \tag{1a}$$

where the two-center Coulomb potential is

$$V(\rho,z)=-[\rho^2+(z+\tfrac{1}{2}R)^2]^{-1/2}-[\rho^2+(z-\tfrac{1}{2}R)^2]^{-1/2}\ . \tag{1b}$$

The coordinate ρ specifies the perpendicular distance of the electron from the internuclear axis and z the projection on that axis, measured from the midpoint between the nuclei; R is the internuclear distance. The squared angular-momentum operator in D dimensions, denoted by l_{D-1}^2, depends on $D-1$ angles Ω_{D-1} and satisfies the equation

$$l_{D-1}^2 Y_{l\{m\}}(\Omega_{D-1})=l(l+D-2)Y_{l\{m\}}(\Omega_{D-1})\ . \tag{2}$$

The eigenfunctions $Y_{l\{m\}}$ are hyperspherical harmonics, the generalized harmonics on a $D-1$ dimensional surface [15]. They can be chosen to diagonalize simultaneously the angular-momentum operators l_{D-1}^2, $l_{D-2}^2,\ldots,l_1^2$ with eigenvalues labeled by the total angular momentum $l=l_{D-1}$ and the multi-index $\{m\}=\{l_{D-2},l_{D-3},\ldots,l_1\}$. For $D=3$, Eq. (2) reduces to the familiar eigenvalue equation for the spherical harmonics $Y_{lm}(\Omega_2)$, with $l=l_2$ and $m=l_1$.

The $D-2$ angles Ω_{D-2} involved in the l_{D-2}^2 operator of Eq. (1) are separable with the ansatz for the wave function

$$\Psi=\rho^{-(D-2)/2}\phi_l(\rho,z;R)Y_{l\{m\}}(\Omega_{D-2})\ . \tag{3}$$

Inserting this into the Schrödinger equation $[h^{\mathrm{TC}}-E(R)]|\Psi\rangle=0$, yields a two-dimensional problem in (ρ,z):

$$\left[-\frac{1}{2}\frac{\partial^2}{\partial\rho^2}-\frac{1}{2}\frac{\partial^2}{\partial z^2}+V(\rho,z)+\frac{m^2(D)-\frac{1}{4}}{2\rho^2}-E(R)\right]\phi(\rho,z;R)=0\ , \tag{4}$$

where $m(D)$ is dimensionally dependent and defined by

$$m(D)\equiv l_{D-2}+\tfrac{1}{2}(D-3)\ . \tag{5}$$

Equation (4) is identical in form to the three-dimensional Schrödinger equation in cylindrical coordinates, with $m(3)=l_1\equiv m$. Consequently, states with the same $m(D)$ quantum number have the same energies $E(R)$ in different dimensions D and the same wave functions $\phi_{m(D)}(\rho,z;R)$. They differ only in $Y_{l\{m\}}(\Omega_{D-2})$, the angular part of the wave function.

The two-center equation for H_2^+ given in Eq. (4) for the cylindrical coordinate system is separable in prolate spheroidal coordinates (λ,μ), related to cylindrical coordinates by

$$\rho=\tfrac{1}{2}R(\lambda^2-1)^{1/2}(1-\mu^2)^{1/2} \tag{6a}$$

and

$$z=\tfrac{1}{2}R\lambda\mu\ . \tag{6b}$$

Hence the wave function is factorizable according to

$$\phi_m(\rho,z;R)=\varphi_{n_\lambda}^m(\lambda;R)\chi_{n_\mu}^m(\mu;R)\ . \tag{7}$$

An H_2^+ electronic eigenstate is then completely classified by three exact spheroidal quantum numbers: n_λ, n_μ and $m(D)$. Here n_λ and n_μ represent the respective number of nodes in the λ and μ coordinates, while $m(D)$ is the sum of l_{D-2}, the number of nodes in the θ_{D-2} coordinate, and a dimensionally dependent term. These quantum numbers may be equivalently expressed by the parabolic quantum numbers that pertain to the separated atom limit: n_1, n_2, and $m(D)$. The correspondence is

$$n_1=n_\lambda\ ,\quad n_2=\left[\frac{n_\mu}{2}\right]\ ,\quad m=m \tag{8}$$

where [ ] denotes the largest integer. We note also that the correspondence with the commonly used spherical quantum numbers (n,l,m) for the united atom limit is $n=n_\lambda+n_\mu+m+1$ and $l=n_\mu+m$. A complete description of an H_2^+ eigenstate including nuclear motion requires three further quantum numbers: J, M, and v, which specify the rotational and vibrational eigenstates for R, the internuclear axis.

B. Saddle properties and near degeneracies

In addition to dimensionally related states with the same n_λ and n_μ but different $m(D)$, H_2^+ has a class of near degenerate states. The corresponding potential curves have different united-atom limits but are close in energy for a large range of internuclear distances, including the separated-atom limit. The near degeneracies of this class of states are attributed to localized motion

about the saddle point $\rho=z=0$ of the two-center potential in three dimensions [2].

Saddle degenerate states are classified according to certain properties. One of these is the quantum number $A=(-1)^{n_\mu}$, which specifies whether the state has a node ($A=-1$) or an antinode ($A=+1$) at the saddle and which consequently divides the entire H_2^+ spectrum into two subspectra based on the amplitude of the wave function at the saddle point of the potential. In addition to having the same value of the A quantum number, states related by saddle degeneracies must converge to the same separated-atom threshold N. The key requirement for saddle degenerate levels, however, is a consequence of the harmonic expansion of the potential $V(\rho,z)$ in Eq. (4) about the saddle point. This leads to a radial Schrödinger equation for an isotropic oscillator in the $D-1$ dimensional subspace perpendicular to the internuclear axis,

$$\left[-\frac{1}{2}\frac{\partial^2}{\partial\rho^2}+\frac{m^2(D)-\frac{1}{4}}{2\rho^2}+\frac{1}{2}\omega^2\rho^2-E\right]\varphi(\rho;R)=0\ , \tag{9}$$

where $\omega=2R^{-3/2}$. The eigenvalues of Eq. (9) are given by [2] $E=\hbar\omega(v_2+1)$, with

$$v_2=2n_\rho+m(D)\ . \tag{10}$$

Here, the quantum number n_λ can be substituted for n_ρ since λ is proportional to ρ in the saddle limit where $\lambda\to1$ and $\mu\to0$, as seen from Eq. (6a). For H_2^+ states to have degenerate eigenvalues within the saddle expansion, it is necessary that they have identical v_2 quantum numbers. Since v_2 is a function of two quantum numbers, H_2^+ states with different (n_λ,m) but the same v_2 can be saddle degenerate. The three properties which specify H_2^+ saddle degenerate states—the presence or absence of a node at the saddle point of the potential, convergence to the same separated-atom threshold, and degeneracy of the isotropic oscillator levels—can then be summarized in the three quantum numbers A, N, and v_2.

Since $N=n_1+n_2+m+1$, another convenient way to label saddle degenerates states is to use the separated-atom notation of parabolic quantum numbers $(n_1n_2m)^A$. For example, in three-dimensional space, the states $(006)^{\pm}$, $(114)^{\pm}$, $(222)^{\pm}$, and $(330)^{\pm}$ are saddle degenerate in the $N=7$ manifold with $v_2=6$. In this paper we concentrate on the $A=+1$ spectrum, the states with antinodes at the saddle.

In view of Eq. (5), any set of saddle degenerate states can also be described as arising from interdimensional degeneracies among σ states ($l_{D-2}=0$). For the example just mentioned, the four saddle degenerate states correspond to $D=15$, 11, 7, and 3, respectively. Table I lists all the sets of saddle degenerate states that occur in three dimensions for $N\le5$, with the corresponding values of D (at right) for σ states. In addition to the parabolic quantum numbers, the customary united-atom labels are shown. Within any set of saddle degenerate states $\Delta n_1=\Delta n_2=-1$, $\Delta m=2$, and $\Delta D=4$. These molecular quantum numbers are directly related [2] to the quantum numbers $K=n_2-n_1$ and $T=m$, which are widely used in the hyperspherical treatment of two-electron atomic states [8–10]. Since $v_2=N-K-1$, within any set of saddle degenerate states $\Delta K=0$ and $\Delta T=2$.

TABLE I. Saddle and interdimensional degeneracies of H_2^+ electronic states arising from separated atom manifolds with principal quantum number N.

N	n_1 n_2 m	$A=+1$	$A=-1$	v_2	K	D
3	1 1 0	$4d\sigma_g$	$5f\sigma_u$	2	0	3
	0 0 2	$3d\delta_g$	$4f\sigma_u$	2	0	7
4	1 2 0	$6g\sigma_g$	$7h\sigma_u$	2	1	3
	0 1 2	$5g\delta_g$	$6h\delta_u$	2	1	7
	1 1 1	$5f\pi_u$	$6g\pi_g$	3	0	5
	0 0 3	$4f\phi_u$	$5g\phi_g$	3	0	9
	2 1 0	$5d\sigma_g$	$6f\sigma_u$	4	−1	3
	1 0 2	$4d\delta_g$	$5f\delta_u$	4	−1	7
5	1 3 0	$8i\sigma_g$	$9k\sigma_u$	2	2	3
	0 2 2	$7i\delta_g$	$8k\delta_u$	2	2	7
	1 2 1	$7h\pi_u$	$8i\pi_g$	3	1	5
	0 1 3	$6h\phi_u$	$7i\phi_g$	3	1	9
	2 2 0	$7g\sigma_g$	$8h\sigma_u$	4	0	3
	1 1 2	$6g\delta_g$	$7h\delta_u$	4	0	7
	0 0 4	$5g\gamma_g$	$6h\gamma_u$	4	0	11
	2 1 1	$6f\pi_u$	$7g\pi_g$	5	−1	5
	1 0 3	$5f\phi_u$	$6g\phi_g$	5	−1	9
	3 1 0	$6d\sigma_g$	$7f\sigma_u$	6	−2	3
	2 0 2	$5d\delta_g$	$6f\delta_u$	6	−2	7

In the approximation of Eq. (9), the saddle states with $m>0$ are doubly degenerate, corresponding to the $\pm m$ azimuthal degeneracy of the oscillator. This degeneracy will be lifted by coupling with overall rotation, to give a pair of near-degenerate states with the same value of v_2 and m but different parity, as in the "Λ doubling" which occurs for excited states of the degenerate bending vibration of a linear molecule [16]. Since in such states the molecule can be regarded as bent on the average, this doubling can also be attributed to "asymmetry splitting" of a slightly asymmetric rotor. If the total electronic angular momentum is L, the pair of near degenerate states may be designated $L_{m,L-m}$ and $L_{m,L-(m-1)}$, in asymmetric-rotor notation [16]. This convenient notation also connects naturally with the large-D limit, which gives "bent" electronic structures for both the H_2^+ system [4] and for the two-electron atom [13].

Figure 1 displays (at left) the systematics of the quantum numbers for the two-center Coulomb problem in "diamond digrams" analogous to the "I supermultiplets" (at right) used by Herrick, Kellman, and Poliak [6] to classify intrashell doubly excited states of two-electron atoms. In this format, nearly degenerate saddle states or asymmetry doublets appear on the same horizontal within each diamond. States with given m or σ states with given D appear on the same vertical. The saddle states of Table I appear in the main torso of each diamond. Other states in each N multiplet which have solo values of v_2 appear in top and bottom "caps" with $m=0$ or 1 and $|K|=N$ or $N-1$. The molecular and atomic patterns are isomorphic.

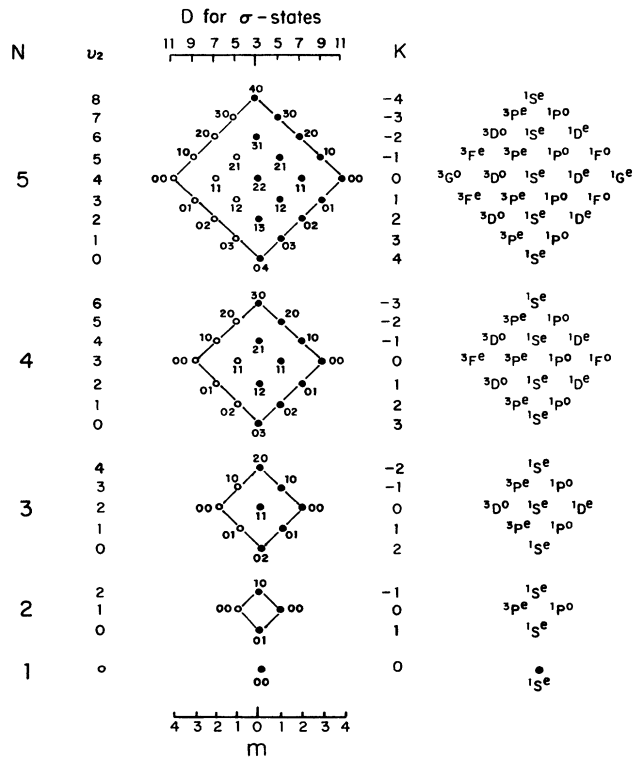

FIG. 1. Supermultiplet display of H_2^+ states (at left) labeled by parabolic quantum numbers (n_1,n_2) and by the projection m (for $D=3$) of the electronic angular momentum in the internuclear axis. The dimensions D corresponding to $m=0$ states are also indicated as well as other quantum numbers that specify the separated atom shell: $N=n_1+n_2+m+1$, the Stark projection $K=n_2-n_1$, and the saddle excitation $v_2=2n_1+m$. Isomorphic supermultiplets are shown (at right) for corresponding intrashell doubly excited states of two-electron atoms.

III. MOLECULAR DESCRIPTION OF TWO-ELECTRON STATES IN ARBITRARY DIMENSIONS

The remarkable symmetries exhibited by the H_2^+ molecular spectrum can be used to interpret the pattern of quasidegenerate doubly excited atomic states. The molecular symmetries provide a simple and appealing interpretation of the atomic spectra because the atomic states can be described in terms of adiabatic MO potentials, as demonstrated in recent work [2,17]. Here we only state the known results but emphasize the new modifications resulting from D-dimensional generalization. In particular, we demonstrate how the molecular description of the complete three-body motion affects H_2^+ interdimensional degeneracies.

The D-dimensional motion of two electrons in the field of an infinitely heavy nucleus of charge Z is described by the Hamiltonian

$$H=-\nabla_R^2-\frac{1}{4}\nabla_r^2-\frac{1}{r_1}-\frac{1}{r_2}+\frac{1}{ZR}\ , \tag{11}$$

where we use molecular Jacobian coordinates. These coordinates are related to the electron-nucleus vectors $\mathbf{r}_i$ by $\mathbf{R}=\mathbf{r}_1-\mathbf{r}_2$, and $\mathbf{r}=\frac{1}{2}(\mathbf{r}_1+\mathbf{r}_2)$. All lengths in Eq. (11) are scaled by the nuclear charge via $x=Zx'$, and energy is scaled according to $E=E'/Z^2$, where primed quantities are in atomic units. The D-dimensional Laplacian operators are given by

$$\nabla_R^2=\sum_{i=1}^{D}\frac{d^2}{dX_i^2}=\frac{1}{R^{D-1}}\frac{\partial}{\partial R}R^{D-1}\frac{\partial}{\partial R}-\frac{\mathcal{L}_{D-1}^2}{R^2} \tag{12a}$$

and

$$\nabla_r^2=\sum_{i=1}^{D}\frac{d^2}{dx_i^2}=\frac{1}{r^{D-1}}\frac{\partial}{\partial r}r^{D-1}\frac{\partial}{\partial r}-\frac{l_{D-1}^2}{r^2}\ , \tag{12b}$$

where $\mathcal{L}_{D-1}^2$ and l_{D-1}^2 are the analogous D-dimensional angular-momentum operators. These are specified further in the Appendix. We can now recast the dimensionally generalized two-electron atomic problem into a dimensionally generalized molecular problem by an ansatz for the spatial wave function:

$$\psi^{L\{M\},S,\pi}(\mathbf{r},\mathbf{R})=\sum_{i,\{m\}}\mathcal{D}^{L,S,\pi}_{\{M\}\{m\}}(\Omega_{D-1})F_i(\tilde{R})\tilde{R}^{-(D-1)/2}\times\phi_{i,\{m\}}(\tilde{\mathbf{r}};\tilde{R})\ , \tag{13}$$

where the tilde denotes body-fixed quantities. This D-dimensional generalization of the molecular two-electron wave function is similar to its three-dimensional prototype [1]. As in $D=3$, the wave function of Eq. (13) is an eigenfunction of the *exact* two-electron symmetry operators, spin (S) and parity (π), as well as of the *total* orbital angular-momentum operator L_{D-1}^2 with quantum number L. In D dimensions, however, there is an additional set of $D-3$ angular-momentum operators $(L_{D-2}^2,L_{D-3}^2,\ldots,L_1^2)$ which all commute with the Hamiltonian of Eq. (11). The quantum numbers for these operators are condensed in the multi-index $\{M\}=\{L_{D-2},L_{D-3},\ldots,L_1\}$ where $L_1\equiv M$ is the familiar projection of the angular momentum onto the space-fixed $\hat{x}_3$ axis. This is analogous to Eq. (2).

The sum in Eq. (13) consists of the products of three terms. The first factor $\mathcal{D}$ is a linear combination of generalized rotation matrices (described in the Appendix) parametrized by a set of $D-1$ Euler angles Ω_{D-1}. Construction of $\mathcal{D}$ as a linear combination of the matrices guarantees that the complete wave function ψ is an eigenfunction of the spin and parity operators [18]. The factor $\mathcal{D}$ rotates the space-fixed coordinate frame S into a body-fixed frame $\tilde{S}$ which is defined such that the interelectronic vector $\tilde{\mathbf{R}}$ lies along the body-fixed $\hat{x}_D$ axis. The other two terms in Eq. (13) represent the body-fixed two-electron wave function. $F_i(\tilde{R})/\tilde{R}^{(D-1)/2}$ corresponds to interelectronic vibration, and the wave function $\phi_{i,\{m\}}(\tilde{\mathbf{r}};\tilde{R})$ is the solution of Eq. (3) of the H_2^+ two-center problem. Choosing the separable two-center molecular wave function of Eq. (3) for $\phi_{i,\{m\}}(\tilde{\mathbf{r}};\tilde{R})$ in Eq. (13) is the key to the molecular characterization of two-electron states. This choice allows us to restrict the expansion on the right-hand side of Eq. (13) to one single

channel $i,\{m\}$,

$$\psi_{i,\{m\}}^{L\{M\},S,\pi}(\mathbf{r},\mathbf{R}) = \mathcal{D}_{\{M\}\{m\}}^{L,S,\pi}(\Omega_{D-1})F_i(\tilde{R})\tilde{R}^{-(D-1)/2}\phi_{i,\{m\}}(\tilde{\mathbf{r}};\tilde{R}) . \quad (14)$$

In the following, we drop the tilde symbol in denoting body-fixed quantities, because henceforth we will *always* work in the body-fixed frame.

Upon first consideration, the single-channel molecular ansatz of Eq. (14) may not seem to be a suitable approximation, especially in higher dimensions, since the exact wave function includes a sum over all orientations $\{m\}$ and all channels i of $\phi_{i,\{m\}}(\mathbf{r};R)$. However, the single-channel molecular approximation in three dimensions yields reasonable values for the two-electron energies of symmetric doubly excited states [2], indicating that the wave function of Eq. (14) correctly accounts for electronic density in the major part of the Hilbert space associated with these states. Furthermore, the H_2^+ nodal lines along fixed λ and μ of Eq. (14) explain the nodal patterns found in the probability density of doubly excited states [17].

Moreover, generalization of the single-channel molecular ansatz to D dimensions provides further justification for the molecular description of two-electron atomic states. We show that this simple, almost analytic molecular approximation of Eq. (14) can explain similarities and exact degeneracies of two-electron levels of different angular momenta or, equivalently, in different dimensions. We first project the Schrödinger equation $(H-E)|\psi\rangle=0$ onto the known part of the D-dimensional molecular two-electron wave function of Eq. (14) in the $2D-1$ variables $(\mathbf{r},\Omega_{D-1})$. The $2D$-dimensional problem then reduces to a one-dimensional differential equation for interelectronic vibration,

$$\left[-\frac{d^2}{dR^2}+V(R)+\frac{1}{ZR}-E\right]F(R)=0 . \quad (15a)$$

Solutions of Eq. (15a) form series of two-electron levels converging to the hydrogenic threshold N associated with the particular $V(R)$. The intrashell levels, which are our main focus, are vibrational ground-state energies for different potentials. The two-electron potential $V(R)$ contains all the D-dimensional dynamics and can be written as a sum of two terms:

$$V(R)=V_3(R)+\frac{(D-3)(D-5)}{4R^2} . \quad (15b)$$

Here $V_3(R)$ is a generalization of the well-known potential in *three* dimensions [2],

$$V_3(R)=E_{m(D)}(R)+\langle\phi_{m(D)}| -\frac{d^2}{dR^2}+\frac{l_x^2+l_y^2}{R^2}+\frac{1}{4}\nabla_r^2|\phi_{m(D)}\rangle + \frac{L(D)[L(D)+1]-m(D)^2}{R^2} , \quad (15c)$$

with $E_{m(D)}(R)$ the eigenvalue of Eq. (4). The D dependence of $V_3(R)$ thus is confined to the angular-momentum quantum numbers

$$L(D)=L+\tfrac{1}{2}(D-3) , \quad m(D)=l_{D-2}+\tfrac{1}{2}(D-3) . \quad (15d)$$

Equations (15) are derived in the Appendix.

Without the second term in Eq. (15b) there would be exact interdimensional degeneracies within the single-channel approximation for states connected by the usual "dimensional link" [19]

$$(D,L)\leftrightarrow(D-2i,L+i) , \quad i=0,1,2,3,\ldots . \quad (16)$$

Even with the presence of the D-dependent centrifugal barrier $\frac{1}{4}(D-3)(D-5)/R^2$ in Eq. (15b), interdimensional degeneracies still occur for potentials which satisfy the additional requirements that the barrier has the same value for D and $D-2i$ as described in Eq. (16). Due to the restriction $D\geq 3$ imposed by the term V_3 in Eq. (15b), these states are limited to members of the set $(D=3,D=5)$. This degeneracy is well known from Herrick's work [12].

Although it destroys many H_2^+ interdimensional degeneracies, the analytic dependence of the interelectronic potential $V(R)$ on D allows us to make *quantitative* predictions about the interdimensional similarities of two-electron states. Consider two series of states in different dimensions D,D', linked by the transcription of Eq. (16), $D=D'-2i$. The potentials $V(R)$ and $V'(R)$ of these states differ only in the D dependent angular-momentum barrier described in Eq. (15b). The difference in the barrier is quadratic in i but linear in D. Thus, when we go to higher-dimension D, interdimensional similarities are better preserved for the case where D' also increases and i remains fixed than for the counter example where i increases while D' is constant. However, we primarily consider the second case, since we wish to approximate high-angular-momentum states in $D'=3$ using $L=0$ states in higher dimension D. As illustrated in Sec. IV, we find that deviations of the $^1S^e$ intrashell levels for $D\leq 11$ from their corresponding energies in $D'=3$ and $L\leq 4$ do not exceed 4%. Essentially, the single-channel MO approximation of two-electron motion shows exact degeneracies between energy levels in $D'=3$ and 5 and similarities of variable degree between other dimensionally related states.

IV. QUASIDEGENERACIES OF INTRASHELL DOUBLY EXCITED ATOMIC STATES

Within the single-channel molecular approximation, we can organize the doubly excited atomic energies into multiplets. Furthermore, applying the interdimensional and saddle degeneracies in H_2^+ potential curves to the two-electron atom unifies different aspects of the two-electron spectrum which have been studied using various approaches [1,2,5–13]. We will use the interdimensional relations of Sec. III to define "generator" $^1S^e$ potentials in $D\geq 3$. These D-dimensional MO's can each be uniquely related to a group of three-dimensional MO potentials which give rise to quasidegenerate atomic intrashell levels. Thus the complex spectrum of two-electron intrashell levels is greatly simplified to generator $^1S^e$ states in

dimensions $D \geq 3$. The generator potentials are defined by the molecular quantum numbers $(n_1 n_2 m(D))^A$, where $m(D)=(D-3)/2$ and either n_1 or n_2 or both are zero. Thus, in the diagrams of Fig. 1, the corresponding generator states are located along the edges of each diamond. Since they are of $^1S^e$ symmetry, the generator potentials for $A=+1$ states can be completely characterized by the dimension D and the quantum number $K=n_2-n_1$, where $D \geq 3$ and K runs from $-N$ to $+N$ in integer steps.

For each of the generator potentials the corresponding group of quasidegenerate two-electron potentials in $D=3$ can be identified in three steps given below. For clarity, we also outline properties of a specific example, the generator potential with $D=7$ and $K=0$.

(i) Select the angular momentum for the $D=3$ MO which connects it with the generator MO in D according to the transcription of Eq. (16). The angular momentum for $D=3$ which corresponds to the $K=0$ state in $D=7$ is $L=m=2$. Thus, since $K=0$ implies $n_1=n_2=0$, this generator's *dimensionally related* MO in $D=3$ is $(002)^+$ in the separated-atom notation. For this state $N=3$.

(ii) Find the other MO potentials which are *saddle degenerate* with the dimensionally related MO. The only saddle degenerate MO for $(002)^+$ in the manifold $N=3$ with $v_2=m=2$ is $(110)^+$ with $v_2=2n_1=2$ and $L=m=0$.

(iii) Construct the two-electron atomic states which originate from each saddle degenerate MO. In general, due to the Λ doubling, there will be two quasidegenerate atomic levels of the same vibrational excitation but opposite spin and parity associated with each MO potential. For our example, we obtain the $(^1D^e, ^3D^o)$ pair from $(002)^+$ but only a $^1S^e$ state from $(110)^+$, since the $^3S^o$ symmetry is forbidden.

We are now able to construct complete groups of quasidegenerate intrashell energy levels because these three steps account for the three known types of approximate or exact degeneracies: (i) the interdimensional degeneracy, (ii) the saddle degeneracy; and (iii) the molecular Λ-doubling or "asymmetry-doublet" degeneracy.

Figure 2 exhibits quasidegenerate excited $D'=3$ energy levels of helium with $N \leq 5$ and $L \leq 4$ which correspond to $^1S^e$ intrashell levels for $D=3$, 5, 7, 9, and 11. Again we use the diamond supermultiplet format to display the $D'=3$ states. However, only the $K=0$ and -1 states are shown since at present D-dimensional energies are available only for these intrashell states. Table II lists both the energies of the $D'=3$ [20–24] states and the corresponding $^1S^e$ generator states for $K=0$ and -1; these arise from nominal $1s^2$ and $2p^2$ configurations, respectively, but configuration mixing is large, especially for $N>1$. The energies $E_D(K)$ of the $K=0$ generator states have been calculated to eight or more significant figures by both variational [25] and perturbation [14,26,27] techniques. To a fair approximation, these energies can be obtained by simply combining first-order perturbation calculations about the $D \to 1$ and ∞ limits [28]; this gives

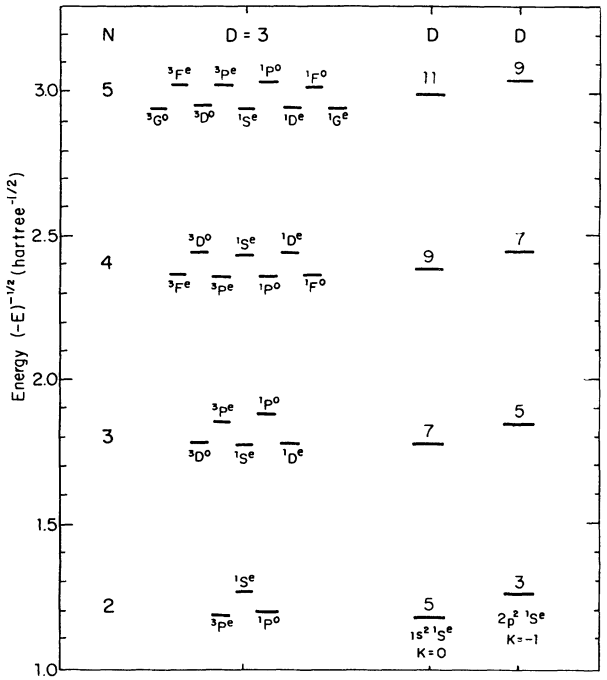

FIG. 2. Correlation of quasidegenerate excited $D'=3$ energy levels of helium with $K=0$ or -1 (at left, format as in Fig. 1) with corresponding $^1S^e$ "generator states" for $D=3,5,7,9,11$ (at right). Ordinate scale plots $(-E)^{-1/2}$, where E (in hartree atomic units) is energy below the double-ionization limit $(He^{2+}+2e^-)$. Energies and MO designations are given in Table II.

$$E_D(K=0)=-[2Z/(D-1)]^2[0.788\,85-0.079\,11(1-\delta)-0.025\,92(1-\delta)^2+0.015\,81\delta(1-\delta)^2+\cdots],$$

with $\delta=1/D$; the accuracy is 0.14% for $D=3$ and improves as D increases. The energies $E_D(K)$ of the $K=-1$ generator states are from similar dimensional perturbation calculations [26].

Figure 3 plots the ratio of the energies for each of the quasidegenerate states and the generator state of the appropriate dimension, specified by $2N+1=D+2|K|$. Although the deviation from unity of these normalized energies increases with D, the discrepancy is less than 4% up to $D=11$. The normalized energies increase with D because the centrifugal term in Eq. (15b) causes the interdimensional degeneracies to become progressively less

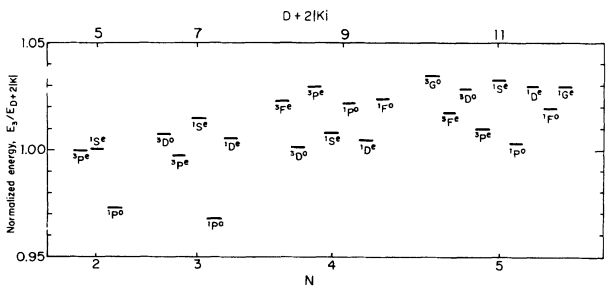

FIG. 3. Energies of quasidegenerate $D'=3$ helium states normalized to corresponding generator state. Format as in Figs. 1 and 2.

TABLE II. Quasidegenerate helium intrashell levels and corresponding generator levels in higher dimensions.

N	$(n_1,n_2,m)^A$	$^{2S+1}L^{\pi}$	$-E_3$	$-E_D(K=0)$	$-E_D(K=-1)$	$D+2\|K\|$
1	$(0,0,0)^+$	$^1S^e$	2.9037	2.9037		3
2	$(0,0,1)^+$	$^3P^e$	0.7105[a]	0.7105		5
		$^1P^o$	0.6913[b]			
	$(1,0,0)^+$	$^1S^e$	0.6219[c]		0.6216	
3	$(0,0,2)^+$	$^3D^o$	0.3151[d]	0.3127		7
		$^1D^e$	0.3145[d]			
	$(1,1,0)^+$	$^1S^e$	0.3175[c]			
	$(1,0,1)^+$	$^3P^e$	0.2907[e]		0.2913	
		$^1P^o$	0.2820[e]			
4	$(0,0,3)^+$	$^3F^e$	0.1789[f]	0.1749		9
		$^1F^o$	0.1791[f]			
	$(1,1,1)^+$	$^3P^e$	0.1802[g]			
		$^1P^o$	0.1788[e]			
	$(1,0,2)^+$	$^3D^o$	0.1671[f]		0.1667	
		$^1D^e$	0.1676[f]			
	$(2,1,0)^+$	$^1S^e$	0.1682[g]			
5	$(0,0,4)^+$	$^3G^o$	0.1154[f]	0.1115		11
		$^1G^e$	0.1149[f]			
	$(1,1,2)^+$	$^3D^o$	0.1147[f]			
		$^1D^e$	0.1149[f]			
	$(2,2,0)^+$	$^1S^e$	0.1152[c]			
	$(1,0,3)^+$	$^3F^e$	0.1094[f]		0.1075	
		$^1F^o$	0.1096[f]			
	$(2,1,1)^+$	$^3P^e$	0.1087[g]			
		$^1P^o$	0.1079[g]			

[a]Reference [11].
[b]Reference [20].
[c]Reference [21].
[d]Reference [22].
[e]Reference [23].
[f]Reference [24].
[g]Reference [6]; derived by graphical estimation of shift from neighboring levels with same N and K.

rigorous as D becomes larger. On the other hand, the saddle degeneracies and the near coincidence of asymmetry doublets become more accurate for higher quantum numbers.

V. DISCUSSION

The dimensionally generalized molecular-orbital description of two-electron states proves to be efficient because the D dependence can be condensed into a simple analytic form contained in the adiabatic MO potential. This provides a systematic procedure for analysis of observed similarities among two-electron potential curves derived from the hyperspherical method [10] as well as elucidating other quasidegeneracies among doubly excited two-electron states.

Correlated two-electron motion is often described by hyperspherical potential curves $V(\Re)$, in terms of the hyperradius $\Re=(r_1^2+r_2^2)^{1/2}$. These curves can be uniquely associated [1] with MO potential curves $V(R)$ which are functions of the interelectronic distance R, as specified in Eq. (15). Lin first noticed that certain hyperspherical potential curves are remarkably similar in shape [10]. Goodson *et al.* ascribed these similarities to interdimensional degeneracies [11], with the added assumption that the wave function does not change appreciably as D goes from 3 to 5.

The molecular-orbital description adds legitimacy to this assumption, because each pair of similar two-electron potentials can be characterized by the *same* n_λ,n_μ quantum numbers, regardless of the dimension. Consequently, states based on similar two-electron curves but associated with different angular-momentum quantum numbers $L(D)$ and $m(D)$ have the same internal correlation pattern. The formal relation between the quantum numbers of the corresponding potential curves in $D=3$ can be written as

$$^{1,3}L^{\pi}(n_1,n_2,m)^A \leftrightarrow {}^{3,1}(L+1)^{\pi}(n_1,n_2,m+1)^A , \tag{18}$$

where $\pi=(-1)^L$. Application of the "dimensional link" of Eq. (16) to the second state in Eq. (18) results in the ex-

actly degenerate state in $D=5$ with the same quantum numbers n_1 and n_2 as the first state of Eq. (18) has in $D=3$. The identical nodal structure of these dimensionally transformed states explains why the potentials of the original $D=3$ pair of curves have similar shape.

For example, one of the pairs of similar potential curves which satisfies Eq. (18) is composed of the ${}^1S^e(0,2,0)^+$ curve in the $(N=3)$ manifold and the ${}^3P^e(0,2,1)^+$ curve in the $(N=4)$ manifold. The correspondence of Eq. (18) derived from the molecular nodal structure of two-electron states is also valid for higher quantum numbers n_1, n_2, m, and L. Figure 4 shows two examples of related pairs of curves.

The similar shape of such pairs of MO potential curves can be demonstrated more effectively by utilizing dimensional scaling. This is illustrated in Fig. 5, which shows that the scaled curves nearly coincide over a wide range of R. The scaling [27–30] accommodates the singularity structure of the two-center Hamiltonian h^{TC} as a function of dimension. The scaled energy and distance are specified by

$$V_s=\alpha V\ ,\quad R_s=R/\beta\ , \tag{19a}$$

where

$$\alpha=2N^2\ ,\quad \beta=D(D-1)/6\ . \tag{19b}$$

The α factor removes a Coulombic pole in the energy at the $D\to 1$ limit [28]; the β factor scales the distance linearly in $(D-1)$ and quadratically in D for small and large D, respectively [29]; β becomes unity for $D=3$. For the states considered in Figs. 4 and 5, the correspondence between D and the m quantum number gives simply $\alpha=18$ and 32, and $\beta=1$ and $\frac{20}{6}$.

The "dimensional link" stated in Eq. (16) definitively connects dimension and angular momentum, thereby imposing exact hydrogenlike degeneracies between MO potentials in different dimensions. Most of these degeneracies are lifted when the MO approximation is applied to two-electron motion, since the presence of a second angular-momentum operator limits exact degeneracies for *two-electron* MO potentials to $D=3$ and 5. Yet other dimensionally linked potentials are still approximately

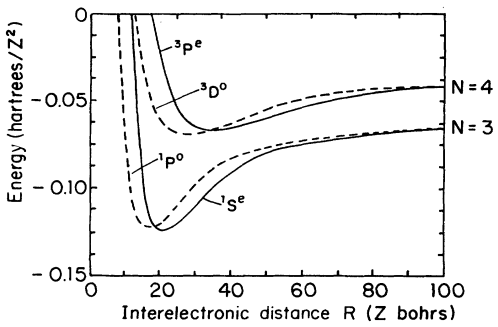

FIG. 4. Two-electron MO potentials of Eq. (15b) for pairs of states $(D=3)$ related by dimensional transcriptions. Solid curves for ${}^1S^e(0,2,0)^+$ and ${}^3P^e(0,2,1)^+$ states and dashed curves for ${}^1P^o(0,1,1)^+$ and ${}^3D^o(0,1,2)^+$ states, in the notation of Eq. (18): ${}^{2S+1}L^{\pi}(n_1,n_2,m)^A$. Distance and energy units are scaled by nuclear charge Z as in Eq. (11).

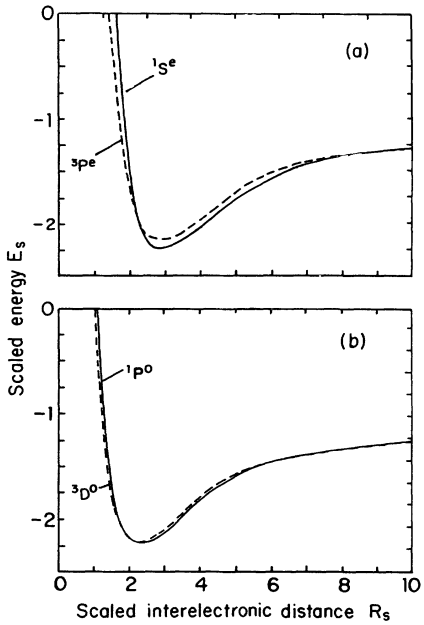

FIG. 5. Two-electron MO potentials of Fig. 4 scaled according to Eq. (19), for pairs of dimensionally related states: (a) ${}^1S^e(0,2,0)^+$ and ${}^3P^e(0,2,1)^+$ states, and (b) ${}^1P^o(0,1,1)^+$ and ${}^3D^o(0,1,2)^+$ states.

degenerate. Our motivation for defining generator ${}^1S^e$ MO potentials in $D\geq 3$ was to create a simple classification scheme capitalizing on these degenerate and near-degenerate relationships. Each generator characterizes a specific group of doubly excited two-electron levels in $D=3$ with various angular momenta and symmetries. Thus the generator states simplify the seeming disarray of doubly excited resonance energies.

Our discussion here is restricted to the single-channel MO approximation and the interdimensional degeneracies associated with it. However, we emphasize that the general approach based on Eq. (13) is a promising method for finding *all exact* interdimensional degeneracies of three-body systems interacting via pairwise forces [18]. The utility of the D-dimensional MO description in elucidating rotational properties of such systems stems from the inherent nexus between dimension and angular momentum.

ACKNOWLEDGMENTS

We thank David Goodson for providing us with results of his D-dimensional two-electron energies. J.M.R. gratefully acknowledges financial support from DAAD-NATO. This work was supported in part at Harvard by the Office of Naval Research and at Freiburg by the DFG under Sonderforschungsbereich 276.

APPENDIX

Before deriving the single-channel adiabatic potential of Eq. (15b) in D dimensions, we briefly review necessary results from D-dimensional angular-momentum algebra

[31] and from the theory of representations of the rotational group in D dimensions [32].

(i) The angular-momentum components are generally defined as elements of a second-rank tensor

$$L_{ij}=x_i p_j - x_j p_i \ , \tag{A1}$$

which are antisymmetric and Hermitian, $L_{ij}=-L_{ji}=L_{ij}^{\dagger}$.

(ii) The tensors (A1) form a linear space. In particular, the sum $L_{ij}=l_{ij}+\mathcal{L}_{ij}$ is an angular-momentum operator if both its components l_{ij} and $\mathcal{L}_{ij}$ are angular-momentum operators. This is a direct consequence of the linearity of the commutator that defines the angular-momentum Lie algebra,

$$[L_{ij},L_{kl}]=i\hbar L_{ik}\delta_{jl} \ . \tag{A2}$$

(iii) A scalar product is defined by contracting

$$L_{D-1}^2=\tfrac{1}{2}\sum_{i,j=1}^{D} L_{ij}L_{ij}^{\dagger}=\tfrac{1}{2}\sum_{i,j=1}^{D} L_{ij}^2 \ . \tag{A3}$$

(iv) The eigenfunctions of L_{D-1}^2 are the generalized harmonics $Y_{L\{M\}}(\Omega_{D-1})$, which diagonalize simultaneously *all* angular-momentum operators L_i^2, $i\le D-2$, with eigenvalues

$$L_i^2 Y_{L\{M\}}(\Omega_{D-1})=L_i(L_i+i-1)Y_{L\{M\}}(\Omega_{D-1}) \ , \tag{A4}$$

where $\{M\}=\{L_{D-2},L_{D-3},\ldots,L_1\}$. The quantum numbers obey the chain rule $L\equiv L_{D-1}\ge L_{D-2}\ge\cdots\ge|L_1|$.

(v) The D-dimensional rotation matrix $\mathcal{D}_{\{M\}\{m\}}(\mathcal{R})$ is the irreducible representation of character $(L,0,\ldots,0)\equiv L$ for the unitary operator $D(\mathcal{R})$ that rotates the D-dimensional coordinate system S into the body-fixed coordinate system $\tilde{S}$. The space of the representation L is spanned by the D-dimensional angular-momentum eigenfunctions $|L\{M\}\rangle$ in (A4). A matrix element of D^L in this basis is given by

$$D^L_{\{M\}\{m\}}(\mathcal{R})=\langle L\{M\}|D^L(\mathcal{R})|L\{m\}\rangle \ . \tag{A5}$$

In this form, $D^L_{\{M\}\{m\}}$ is a simultaneous eigenfunction of the total angular-momentum operator L_{D-1}^2 with eigenvalue $L(L+D-2)$ and of all the angular-momentum operators L_i^2, $i\le D-2$, in the space-fixed frame

$$L_i^2 D^L_{\{M\}\{m\}}=L_i(L_i+i-1)D^L_{\{M\}\{m\}} \ , \tag{A6a}$$

and in the body-fixed frame

$$\tilde{L}_i^2 D^L_{\{M\}\{m\}}=L_i(L_i+i-1)D^L_{\{M\}\{m\}} \ . \tag{A6b}$$

(vi) Only L_i^2, $i=D-1$, is a scalar with respect to the scalar product (A3) in D dimensions. Hence L_{D-1}^2 is invariant under rotation $\mathcal{R}$, while the operators L_i^2, $i\le D-2$ are not. Consequently, the eigenvalues for the L_i^2, $i\le D-2$ operators in the space-fixed frame (A6a) are different from those in the body-fixed frame (A6b). The fact that the L_i^2, $i\le D-2$ operators are not scalars is seen from the relation

$$L_{D-1}^2=\tfrac{1}{2}\sum_{i,j}^{D-1} L_{ij}^2+\sum_{i=1}^{D-1} L_{iD}^2\equiv L_{D-2}^2+\sum_{i=1}^{D-1} L_{iD}^2 \ . \tag{A7}$$

The last sum in (A7) is not invariant under rotation of the coordinates. Thus L_{D-2}^2 cannot be.

We now proceed to the derivation of the single-channel adiabatic potential given in Eq. (15b). This potential is the expectation value

$$V(R)=\left\langle\Phi\left|\frac{\mathcal{L}_{D-1}^2+\frac{1}{4}(D-1)(D-3)}{R^2}+\tfrac{1}{4}\nabla_r^2-\frac{d^2}{dR^2}+h^{\mathrm{TC}}\right|\Phi\right\rangle \ , \tag{A8a}$$

with

$$\Phi=\mathcal{D}^{L,S,\pi}_{lM\{m\}}\phi_{\{m\}}(\mathbf{r};R) \ . \tag{A8b}$$

The wave function $\phi_{\{m\}}$ from Eq. (13) is the eigenfunction of the H_2^+ Hamiltonian h^{TC} in (1). We have suppressed the index i for simplicity. The tensor of *total* orbital angular momentum is the sum of l_{ij} and $\mathcal{L}_{ij}$, which respectively refer to the $\mathbf{r}$ and $\mathbf{R}$ coordinates of Eq. (12),

$$L_{ij}\equiv l_{ij}+\mathcal{L}_{ij} \ . \tag{A9}$$

Since $\mathbf{R}$ lies along the $\hat{x}_D$ axis in the body-fixed frame with $\mathbf{R}=(0,0,\ldots,R)$, it follows from the definition of the angular-momentum tensor (A1) that

$$L_{ij}=l_{ij} \quad \text{for } i,j\le D-1 \ . \tag{A10}$$

Equations (A7), (A9), and (A10) allow us to recast $\mathcal{L}_{D-1}^2$ as

$$\mathcal{L}_{D-1}^2=L_{D-1}^2-L_{D-2}^2+l_{D-1}^2-l_{D-2}^2-\sum_{i=1}^{D-1} L_{iD}l_{iD} \ . \tag{A11}$$

The last sum in (A11) changes the values of the angular-momenta quantum numbers $l_i\in\{m\}$ of $\phi_{\{m\}}(\mathbf{r};R)$. Therefore, this term does not contribute to the expectation value (A8a) for which the set $\{m\}$ represents good quantum numbers. Since Φ from (A8b) is an eigenfunction of L_i^2, the only nontrivial term in (A11) for calculating the expectation value (A8) is $\Delta l^2=\langle\phi_{\{m\}}|l_{D-1}^2-l_{D-2}^2|\phi_{\{m\}}\rangle$. To obtain this term, we expand

$$\phi_{\{m\}}(\mathbf{r},R)=r^{-(D-1)/2}\sum_{l=l_{D-2}}^{\infty} f_l(r,R)|l\{m\}\rangle \ . \tag{A12}$$

Using (A4) and (A12), we obtain

$$\Delta l^2=\sum_{l=l_{D-2}}^{\infty}(l-l_{D-2})(l+l_{D-2}+D-2)\times\int f_l^2(r,R)\,dr+l_{D-2} \ . \tag{A13}$$

Substitution of l and l_{D-2} with $l(D)$ and $m(D)$ analogous to (15d) yields

$$\Delta l^2 = \sum_{l(D)=m(D)}^{\infty} [(l(D)-m(D))][l(D)+m(D)+1] \times \int f^2_{l(D)}(r,R)dr + m(D) - \frac{D-3}{2} . \quad \text{(A14)}$$

Since $l(D)$ and $m(D)$ are invariant under the transcription of Eq. (16) we can finally reduce (A14) to a conventional matrix element in *three* dimensions with a simple D-dependent correction term:

$$\Delta l^2 = \langle \phi_{\{m\}} | l^2_{D-1} - l^2_{D-2} | \phi_{\{m\}} \rangle = \langle \phi_{m(D)}(x,y,z;R) | l_x^2 + l_y^2 | \phi_{m(D)}(x,y,z;R) \rangle - \frac{D-3}{2} . \quad \text{(A15)}$$

As a last step we must show that the expectation value

$$\left\langle \Phi \left| \frac{1}{4}\nabla_r^2 - \frac{d^2}{dR^2} + h^{\mathrm{TC}} \right| \Phi \right\rangle \quad \text{(A16)}$$

can be reduced to its expression in $D=3$. We can rewrite $\frac{1}{4}\nabla_r^2 = -\frac{1}{2}h^{\mathrm{TC}} + V(\rho,z)$ where $V(\rho,z)$ is the potential in (1b) and does not directly depend on the dimension D. Since $d^2/(dR^2)$ also does not affect angular variables, we can integrate (A16) over all angles of dimension $D \geq 4$ to yield the identical matrix element in $D=3$. Combining the results of (A11), (A14), and (A16) leads to the form of the two-electron potential $V(R)$ given in Eq. (15).

*Present address: Departments of Physics and Chemistry, BG-10, University of Washington, Seattle, WA 98195.

[1] J. M. Feagin and J. S. Briggs, Phys. Rev. Lett. **57**, 984 (1986); Phys. Rev. A **37**, 4599 (1988).
[2] J. M. Rost and J. S. Briggs, J. Phys. B **24**, 4293 (1991).
[3] S. M. Sung and D. R. Herschbach, J. Chem. Phys. **95**, 7437 (1991).
[4] D. D. Frantz and D. R. Herschbach, J. Chem. Phys. **92**, 6668 (1990).
[5] M. E. Kellman and D. R. Herrick, Phys. Rev. A **22**, 1536 (1980).
[6] D. R. Herrick and M. E. Kellman, Phys. Rev. A **21**, 418 (1980); D. R. Herrick, M. E. Kellman, and R. D. Poliak, *ibid.* **22**, 1517 (1980).
[7] H. J. Yuh, G. S. Ezra, P. Rehmus, and R. S. Berry, Phys. Rev. Lett. **47**, 497 (1981).
[8] C. D. Lin, Adv. At. Mol. Phys. **22**, 77 (1986).
[9] H. R. Sadeghpour, Phys. Rev. A **43**, 5821 (1991).
[10] C. D. Lin, Phys. Rev. A **29**, 1019 (1984).
[11] D. Z. Goodson, D. K. Watson, J. G. Loeser, and D. R. Herschbach, Phys. Rev. A **44**, 97 (1991).
[12] D. R. Herrick, J. Math. Phys. **16**, 281 (1975).
[13] D. R. Herschbach, J. G. Loeser, and D. K. Watson, Z. Phys. D **10**, 195 (1988).
[14] D. Z. Goodson and D. R. Herschbach, Phys. Rev. Lett. **58**, 1628 (1987).
[15] J. Avery, *Hyperspherical Harmonics: Applications in Quantum Theory* (Kluwer Academic, Dordrecht, 1989).
[16] C. H. Townes and A. L. Schawlow, *Microwave Spectroscopy* (McGraw-Hill, New York, 1955), pp. 32–34, 84–86.
[17] J. M. Rost, R. Gersbacher, K. Richter, J. S. Briggs, and D. Wintgen, J. Phys. B **24**, 2455 (1991); J. M. Rost, J. S. Briggs, and J. M. Feagin, Phys. Rev. Lett. **66**, 1642 (1991).
[18] J. M. Rost (unpublished).
[19] D. R. Herschbach, Faraday Discuss. Chem. Soc. **84**, 465 (1988); At. Phys. **11**, 63 (1989).
[20] Y. K. Ho, Phys. Rev. A **23**, 2137 (1981).
[21] Y. K. Ho, Phys. Rev. A **34**, 4402 (1986).
[22] L. Lipsky, R. Anania, and M. J. Conneely, At. Data Nucl. Data Tables **20**, 127 (1977).
[23] Y. K. Ho and J. Callaway, J. Phys. B **18**, 3481 (1985).
[24] Y. K. Ho, Z. Phys. D **11**, 277 (1989).
[25] J. G. Loeser and D. R. Herschbach, J. Chem. Phys. **84**, 3882 (1986).
[26] D. Z. Goodson and D. K. Watson (unpublished).
[27] M. López-Cabrera, D. Z. Goodson, D. R. Herschbach, and J. D. Morgan III, Phys. Rev. Lett. **68**, 1992 (1992).
[28] D. J. Doren and D. R. Herschbach, J. Chem. Phys. **87**, 433 (1987).
[29] M. López-Cabrera, Ph.D. thesis, University of Michigan, 1991.
[30] D. D. Frantz and D. R. Herschbach, Chem. Phys. **126**, 59 (1988).
[31] J. D. Louck, J. Mol. Spectrosc. **4**, 298 (1960).
[32] M. Hamermesh, *Group Theory* (Addison-Wesley, Reading, MA, 1962).